



# Flywheel Dimensioning

Master's Degree in Automotive Engineering

Loris Fonseca: s342696@studenti.polito.it

Maurizio Pio Vergara: s346643@studenti.polito.it

a.a. 2024/2025

# Contents

<b>1</b>	<b>Introduction</b>	<b>3</b>
<b>2</b>	<b>Analysis of the thermodynamic cycle</b>	<b>3</b>
2.1	Point 1 . . . . .	3
2.2	Point 2 . . . . .	5
2.3	Point 3 . . . . .	5
2.4	Point 4 . . . . .	6
2.5	Plot of the thermodynamic cycle . . . . .	6
<b>3</b>	<b>Single-cylinder engine</b>	<b>6</b>
3.1	Calculation of the imep . . . . .	7
3.2	Calculation of the shaft and resistant moment . . . . .	7
3.3	Calculation of the flywheel diameter . . . . .	10
3.4	Calculation of the instantaneous crankshaft speed . . . . .	12
<b>4</b>	<b>Multi-cylinder engine</b>	<b>12</b>
4.1	Calculation of the shaft and resistant moment . . . . .	13
4.2	Calculation of the flywheel diameter . . . . .	13
4.3	Calculation of the instantaneous crankshaft speed . . . . .	15
<b>5</b>	<b>Conclusions</b>	<b>15</b>
<b>6</b>	<b>Appendix</b>	<b>16</b>

# 1 Introduction

An engine flywheel is a mechanical device used to store kinetic energy, dependent on its inertia moment and angular speed. The aim of the flywheel is to regularize the crankshaft speed, reducing speed oscillations, and so vibrations. The aim of this project is to dimension a flywheel of a Spark Ignition (SI) naturally aspirated engine with port fuel injection. The design is based on the force acting on the piston, thus on the turning moment on the crankshaft. The dimensioning is done considering the worst operating condition, i.e. considering the maximum torque exerted by the engine and with no clutch engaged. Hence:

$$M_{\text{shaft}}(\theta) - M_{\text{load}} = J \frac{d\omega}{dt} \quad (1)$$

$$J = J_{\text{engine}} + J_{\text{flywheel}} \quad (2)$$

The higher is the instantaneous variation of the shaft torque, the larger the flywheel diameter.

## 2 Analysis of the thermodynamic cycle

The first step to perform to evaluate the flywheel diameter is the evaluation of the thermodynamic quantities in the characteristic points of the cycle. In particular, the considered cycle is an air-fuel cycle with the following characteristics:

- Intake and exhaust valves instantaneously open/close at dead centres
- Compression and expansion phases are described as polytropic transformations (with m and m' as polytropic indexes)
- Combustion is diabatic, thus heat transfer occurs
- Combustion and blowdown phases occur at constant volume
- Intake and exhaust phases occur at constant pressure
- No leakages
- Specific heat  $c_p$  and  $c_p'$  are considered as constant

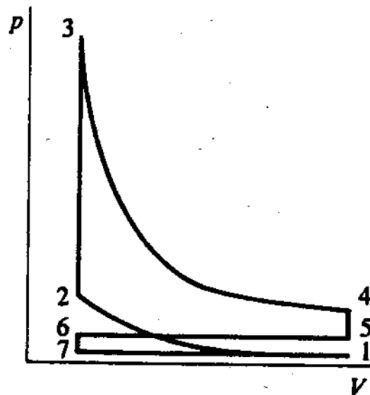


Figure 1: Qualitative representation of an a-f cycle

### 2.1 Point 1

Thermodynamic quantities of point 1 are evaluated through the application of the 1<sup>st</sup> Law of Thermodynamics, between 6 and 1, in the Lagrangian form. Therefore a constant control mass is considered, evaluated as follows:

$$m_1 = m_a + m_f + m_r \quad (3)$$

where  $m_a$  is the mass of air,  $m_f$  the mass of fuel and  $m_r$  the mass of residual gas from the previous cycle. The mentioned principle is reported in Equation 4.

$$Q = W + \Delta U^* + \Delta E_k + \Delta E_g \quad (4)$$

Since we are considering a gas, the density is low, thus the contribution of the gravitational energy can be neglected. Furthermore, during the intake phase, a constant speed can be considered, hence also the variation of the kinetic energy can be neglected. Equation 4 can be simplified as follows:

$$Q = W + \Delta U^* + \cancel{\Delta E_k} + \cancel{\Delta E_g} \rightarrow Q = W + \Delta U^* \quad (5)$$

The work is evaluated starting from its general definition, reported in Equation 6.

$$W = \int_6^1 p dV \quad (6)$$

Two contributions are present: one due to the piston motion, the other due to the environment pressure exerted on the mass.

$$W = \left( \int_6^1 p dV \right)_{\text{external}} + \left( \int_6^1 p dV \right)_{\text{piston}} \quad (7)$$

Therefore, the value of the work can be computed as follows:

$$W = -p_a(m_a V_a + m_f V_f) + p_1(m_a V_{a1} + m_f V_{f1} + m_r V_{r1} - m_r V_{r6}) \quad (8)$$

The variation of internal energy is evaluated through the following equation:

$$\Delta U^* = U_1 - U_6 = m_a(u_{a1} - u_{a6}) + m_f(u_{f1} - u_{f6}) + m_r(u_{r1} - u_{r6}) \quad (9)$$

Therefore, the right-hand-side of Equation 5 can be evaluated, as reported in the following expression:

$$W + \Delta U^* = m_a((u_{a1} + p_1 v_{a1}) - (u_{a6} + p_a v_a)) + m_f((u_{f1} + p_1 v_{f1}) - (u_{f6} + p_a v_{f6})) + m_r((u_{r1} + p_1 v_{r1}) - (u_{r6} + p_1 v_{r6})) \quad (10)$$

It should be noted that the terms in the form  $u + pV$  correspond to the enthalpy of air, fuel and residual gas in points 1 and 6 of the cycle. The only exception is the last term of Equation 10,  $u_{r6} + p_1 v_{r6}$ , which is not equal to the enthalpy of the residual gas in point 6,  $h_{r6}$ , since  $p_1$  is not equal to the residual gas pressure in this point of the cycle. Nevertheless, since this term is small with respect to the other ones, it can be assumed  $p_1 = p_{r6}$  to simplify the equation, still obtaining a low error and a good approximation of the real conditions.

Thus, Equation 10 can be written highlighting the enthalpy terms:

$$W + \Delta U^* = m_a(h_{a1} - h_{a6}) + m_f(h_{f1} - h_{f6}) + m_r(h_{r1} - h_{r6}) \quad (11)$$

which can be rewritten in a form underling the specific heat and the temperature:

$$W + \Delta U^* = m_a c_{p,a}(T_1 - T_{a6}) + m_r c_p'(T_1 - R_{r6}) + m_f c_f(T_1 - T_{f6}) + m_f \cdot x \cdot r \quad (12)$$

It should be noted that the term related to fuel is characterized by two contributions, one due to the latent heat of vaporization ( $r$ ).

The heat contribution of Equation 5 is evaluated as follows:

$$Q = m_a c_{p,a} \Delta T + m_f c_{p,f} \Delta T + m_r c_p' \Delta T \quad (13)$$

where  $Q$  represents the heat required to increase the temperature of the charge of  $\Delta T = 30^\circ$ .

The final expression of the First Principle of Thermodynamic between point 1 and 6 is reported in the following:

$$m_a c_{p,a} \Delta T + m_f c_{p,f} \Delta T + m_r c_p' \Delta T = m_a c_{p,a}(T_1 - T_{a6}) + m_r c_p'(T_1 - R_{r6}) + m_f c_f(T_1 - T_{f6}) + m_f \cdot x \cdot r \quad (14)$$

The temperature in point 1 can be evaluated starting from the just evaluated equation:

$$T_1 = \Delta T + \frac{c_{p,a} \cdot T_a \cdot \alpha + c_p' \cdot T_r \cdot \alpha' + c_f \cdot T_f - x \cdot r}{c_f + \alpha \cdot c_{p,a} + \alpha'} \cdot c_p \quad (15)$$

which gives the following value:

$$T_1 = 330.2 \text{ K}$$

Once the temperature in point one is found,  $p_1$  can be evaluated with the following equation, obtaining starting from Equation 3.

$$p_1 = p_a \left( \lambda_v \cdot (r_c - 1) \cdot \frac{\alpha + 1}{\alpha} \cdot \frac{1}{R T_a} + \frac{p_r}{p_a} \cdot \frac{1}{R' T_r} \right) \cdot \frac{R_1 T_1}{r_c} \quad (16)$$

which gives the following pressure value:

$$p_1 = 88.5 \text{ kPa}$$

## 2.2 Point 2

Considering the assumption made for this study, and reported in Section 2, i.e. that the compression phase from 1 to 2 is considered to be polytropic, characteristic temperature and pressure in point 2 can be simply evaluated by exploiting the equation characterizing this type of transformation:

$$\begin{cases} p_2 = p_1 \cdot r_c^m \\ T_2 = T_1 \cdot r_c^{m-1} \end{cases} \quad (17)$$

from which the following pressure and temperature values are obtained

$$\begin{aligned} p_2 &= 2253 \text{ kPa} \\ T_2 &= 764.3 \text{ K} \end{aligned}$$

## 2.3 Point 3

Pressure and temperature of point 3 can be evaluated by applying the 1<sup>st</sup> Law of Thermodynamics between 2 and 3, in the Lagrangian form. The ideal transformation from 2 to 3 is a constant volume combustion with no heat transfer, which means having a null variation of internal energy.

From this consideration, the following equation can be written:

$$\frac{Q_{LHV,v}(T_2)}{\alpha + 1 + \alpha'} = c_{v'}(T_{3,id} - T_2) \quad (18)$$

However, the real combustion is not ideal, therefore different effects must be taken into account, including: the non null heat transfer, the presence of dissociation, the non completeness of combustion and the presence of excess fuel, i.e. a non stoichiometric mixture.

As a consequence of this non-ideal conditions, Equation 18 must be modified to account also for these effects. Therefore, the following equation is obtained:

$$(1 - \delta_A) \cdot \frac{Q_{LHV,v}(T_2)}{\alpha + 1 + \alpha'} \cdot \frac{\alpha}{\alpha_{st}} = c_{v'}(T_3 - T_2) + d_q(T_3 - T_d)^2 \quad (19)$$

where:

- $(1 - \delta_A)$  is a reduction coefficient accounting for the heat transfer and the incomplete combustion effect
- $\frac{\alpha}{\alpha_{st}}$  accounts for the air-fuel rich mixture
- $d_q(T_3 - T_d)^2$  is the dissociation heat, accounting for the dissociation effect during combustion

The term  $\frac{Q_{LHV,v}(T_2)}{\alpha + 1 + \alpha'}$  represents the lower heating value of the fuel at the temperature  $T_2$ . Since the data provide only the lower heating value at temperature  $T_0 = 288 \text{ K}$ , an equation able to find the one at  $T_2$  must be evaluated. The mentioned equation is the following:

$$\frac{Q_{LHV,v}(T_0)}{\alpha + 1} + c_v(T_2 - T_0) = \frac{Q_{LHV,v}(T_2)}{\alpha + 1} + c_{v'}(T_2 - T_0) \quad (20)$$

from which:

$$Q_{LHV,v}(T_2) = 43402 \text{ kJ/kg}$$

Equation 19 is a second order equation which can be solved in order to find the temperature value in point 3. In particular, it can be written as follows:

$$A \cdot T_3^2 + B \cdot T_3 + C = 0 \quad (21)$$

where:

$$\begin{cases} A = d_q \\ B = c_v' - 2T_d \cdot d_q \\ C = -c_v' \cdot T_2 + d_q \cdot T_d^2 - (1 - \delta_A) \cdot \frac{Q_{LHV,v}(T_2)}{\alpha+1+\alpha'} \cdot \frac{\alpha}{\alpha_{st}} \end{cases} \quad (22)$$

Therefore, the obtained temperature value in point 3 is:

$$T_3 = 2741 \text{ K}$$

Pressure in point 3 can be computed by applying the mass conservation equation, which gives the following formula:

$$p_3 = p_2 \cdot \frac{R_3}{R_2} \cdot \frac{T_3}{T_2} = p_2 \cdot \frac{R'}{R_1} \cdot \frac{T_3}{T_2} \quad (23)$$

from which:

$$p_3 = 8587 \text{ kPa}$$

## 2.4 Point 4

As for point 2, thermodynamic quantities of point 4 are evaluated by applying the characteristic equation of a polytropic transformations, since also the expansion phase is considered to be a polytropic one.

$$\begin{cases} p_4 = p_3 \cdot r_c^{-m'} \\ T_4 = T_3 \cdot r_c^{1-m'} \end{cases} \quad (24)$$

from which the following pressure and temperature values are obtained

$$\begin{aligned} p_4 &= 408.6 \text{ kPa} \\ T_4 &= 1435 \text{ K} \end{aligned}$$

## 2.5 Plot of the thermodynamic cycle

Once all the thermodynamic quantities of the cycle are evaluated, the a-f cycle can be plotted, as shown in Figure 2. It should be noted that  $p_7$  is equal to the pressure in point 1, while  $p_5$  and  $p_6$  are equal to the environmental pressure  $p_a$ .

## 3 Single-cylinder engine

The single-cylinder engine serves as a fundamental model for analyzing engine dynamics and evaluating key design parameters. This section focuses on the detailed calculation of the indicated mean effective pressure (IMEP), the crankshaft and resistant moments, and the dimensioning of the flywheel. These calculations are critical for understanding the performance characteristics and ensuring the smooth operation of the engine under various operating conditions.

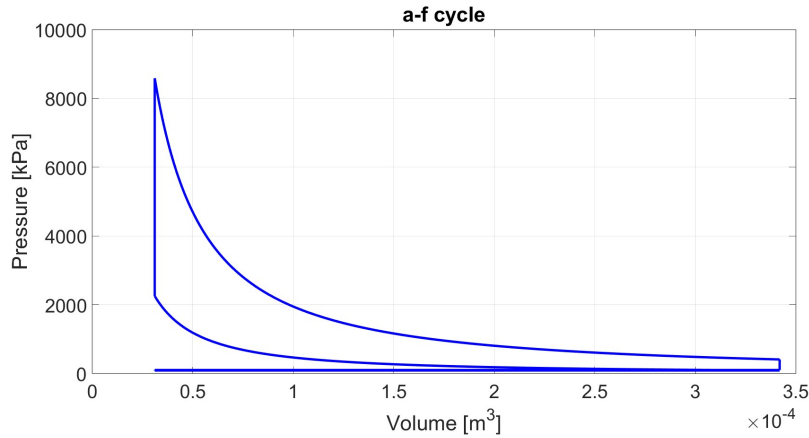


Figure 2: a-f cycle on p-V diagram

### 3.1 Calculation of the imep

The imep of the cycle can be evaluated starting from the general formula defining this quantity, reported below:

$$imep = \frac{\oint dL_i}{V_d} = \frac{\oint p dV}{V_d} \quad (25)$$

Considering the analyzed cycle, the previously reported equation can be written as follows:

$$\frac{1}{V_d} \left( \int_1^2 p dV + \cancel{\int_2^3 p dV} + \cancel{\int_3^4 p dV} + \cancel{\int_4^5 p dV} + \cancel{\int_5^6 p dV} + \cancel{\int_6^7 p dV} + \int_7^1 p dV \right) \quad (26)$$

where the transformation  $2 \rightarrow 3$ ,  $4 \rightarrow 5$  and  $6 \rightarrow 7$  can be eliminated since their contribution is null, being them constant volume transformations. By solving the integrals, the following expression for the *imep* is found:

$$imep = p_1 \cdot \frac{r_c}{r_c - 1} \cdot \frac{1}{1-m} (r_c^{m-1} - 1) + p_3 \cdot \frac{1}{r_c - 1} \cdot \frac{1}{1-m'} (r_c^{1-m'} - 1) + (p_1 - p_r) \quad (27)$$

from which:

$$imep = 10.35 \text{ bar}$$

### 3.2 Calculation of the shaft and resistant moment

Once the data characteristic of the a-f cycle are evaluated, the next step to perform in order to evaluate the flywheel diameter is the evaluation of the crankshaft moment. Firstly, the effective pressure able to generate a moment has to be evaluated, according to the following equation:

$$p_{eff} = p_{gas} - p_c \pm p_i \quad (28)$$

where  $p_{gas}$  is the gas pressure evaluated in Section 2 and reported in Figure 3 as function of the crank angle.

The inertia pressure are evaluated accordingly to the following equation, where the first and second order harmonics are considered:

$$p_i = -\frac{m_{rec}}{V_d} \cdot \frac{\pi^2 u^2}{2} \cdot (\cos \theta + \Lambda \cos 2\theta) \quad (29)$$

Finally, in this study the crankcase pressure  $p_c$  is considered almost equal to the environment one, i.e.  $p_c = 100$  kPa. Therefore, the effective pressure can be evaluated. The resulting plot is reported in Figure 4.

In Figure 5 it is reported the plot showing all the pressure contributions, including the inertia one, as function of the crank angle. Meanwhile Figure 6 depicts the comparison between gas and inertia pressure in the p-V plane.

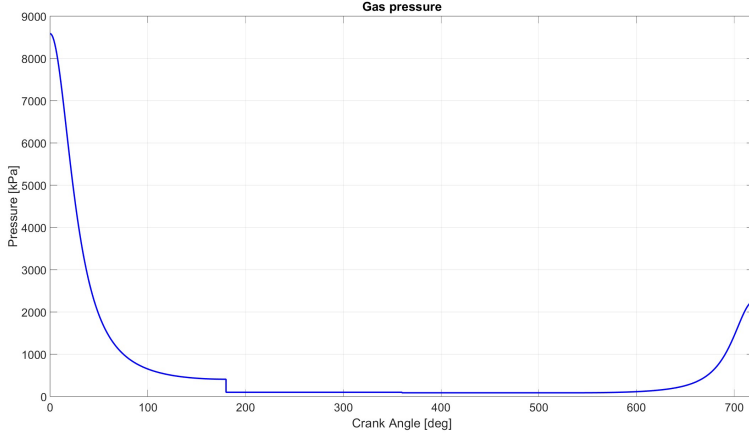


Figure 3: Gas pressure as function of the crank angle

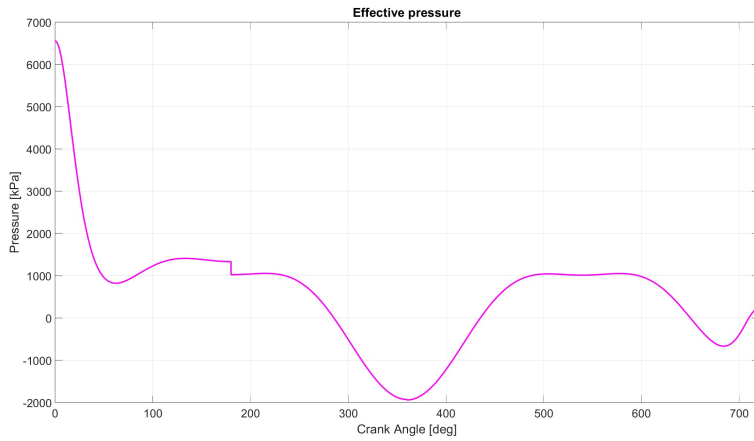


Figure 4: Effective pressure as function of the crank angle

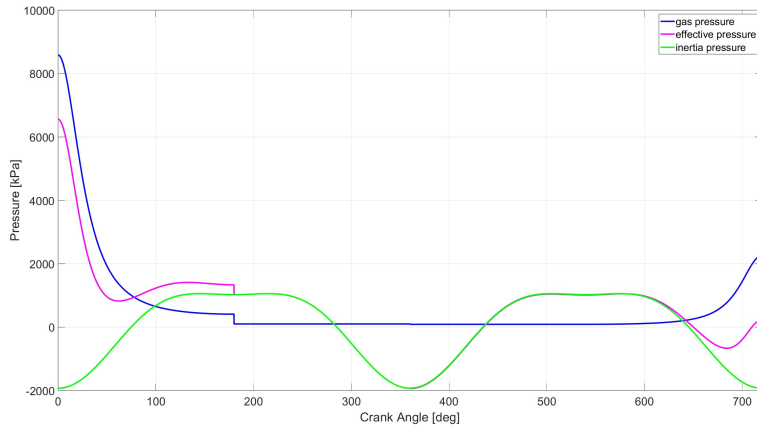


Figure 5: Pressure contributions over the cycle

Evaluating the effective pressure, allows to compute the tangential pressure, which actually is the one contributing to the torque generation. In Figure 7, a simple scheme of force distribution is shown.

By analyzing the picture, it is possible to extrapolate the relationship linking the tangential pressure to the effective one. This relation is reported in Equation 30.

$$p_t(\theta) = p_{eff} \cdot \frac{\sin(\beta + \theta)}{\cos \beta} \quad (30)$$

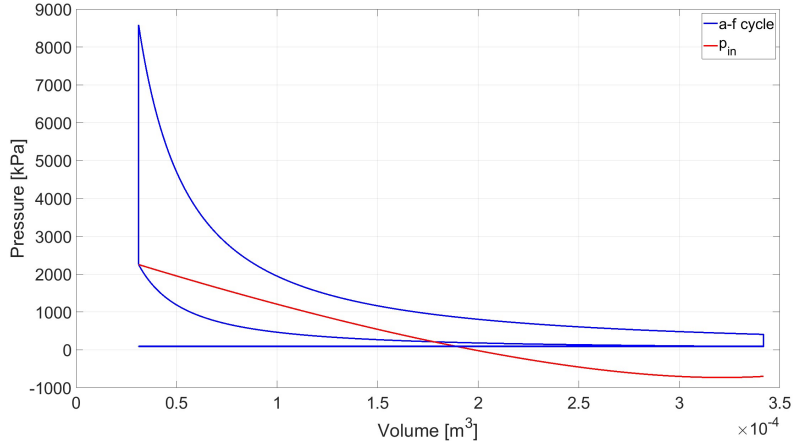


Figure 6: a-f cycle with inertia pressure trend

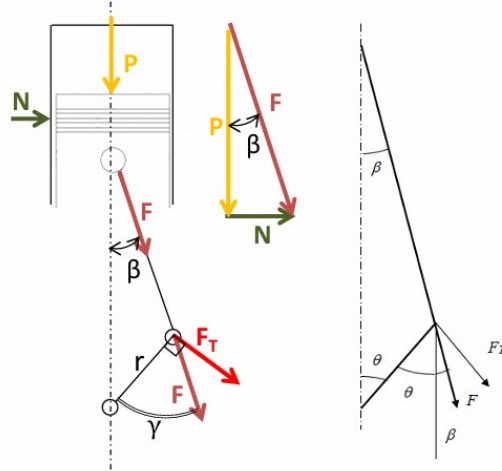


Figure 7: Force distribution

The resulting function of the tangential pressure is reported in Figure 8.

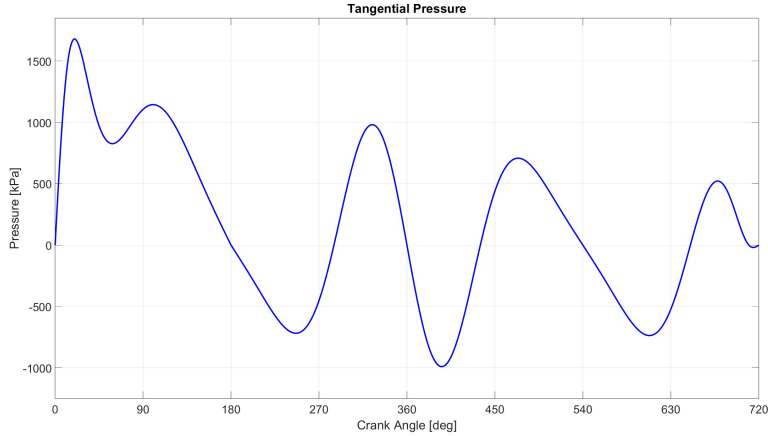


Figure 8: Tangential pressure as function of the crank angle

It should be noted that the tangential pressure is characterized by a null value in correspondance of the Dead Centers, since in these positions the crank and the connecting rod are aligned, hence no torque can be transmitted to the crankshaft. Moreover, discontinuities are expected in the slope of tangential pressure around DCs (except at 540°CA), due to discontinuities in  $p_{eff}$ .

Once the tangential pressure is evaluated, the related crankshaft momentum can be computed

through the following formula:

$$M_s = p_t \cdot \frac{V_d}{2} \quad (31)$$

The resistant moment is evaluated in steady state condition. Therefore, the instantaneous rotational speed of the engine at the beginning of the cycle is equal to the speed at the end of the cycle. As a consequence, the difference between crankshaft and resistant work is null. Moreover, the resistant moment is considered constant over the engine cycle.

$$W_s = W_r = imep \cdot V_d \quad (32)$$

Therefore, the resistant momentum can be evaluated by solving the integral putting in relation the work and the momentum. From this relationship, the following expression for the resistant moment is obtained:

$$M_r = \frac{imep \cdot V_d}{4\pi} \quad (33)$$

from which:

$$M_r = 25.6 \text{ Nm}$$

Once the resistant moment is evaluated, the related resistant pressure can be computed by simply applying the following formula:

$$p_r = \frac{M_r}{\frac{V_d}{2}} \quad (34)$$

which gives the following value of resistant pressure:

$$p_r = 164.7 \text{ kPa}$$

### 3.3 Calculation of the flywheel diameter

The flywheel diameter can be evaluated starting from the value of its inertia  $J_{flw}$ . Since in the engine there is not only the flywheel inertia, all the others contributions have to be considered. Therefore, in general, the total inertia of the system is evaluated as follows:

$$J = J_{eng} + J_{flw} + J_{tran} + J_{user} \quad (35)$$

Since in this survey the engine is considered to be disconnected from the transmission, only the engine and flywheel inertia are taken into account for the evaluation of the total inertia. Therefore,

$$J = J_{eng} + J_{flw} \quad (36)$$

The engine inertia is simply evaluated with the following formula:

$$J_{eng} = m_{rot} \cdot r^2 = \left( \frac{m_{tot}}{iV} \right) V \cdot r^2 \quad (37)$$

which gives:

$$J_{eng} = 4.12 \cdot 10^{-4} \text{ kg} \cdot \text{m}^2$$

Total inertia instead can be evaluated starting from the shaft dynamic equilibrium equation:

$$M_s(\theta) - M_r(\theta) = J \frac{d^2\theta}{dt^2} \quad (38)$$

By integrating two times Equation 38, the following expression for the total inertia is found:

$$J = \frac{\xi \cdot imep \cdot V_d}{\delta \cdot \omega_{avg}^2} \quad (39)$$

where  $\delta$  is the kinematic irregularity, while  $\xi$  is the dynamic irregularity. They are evaluated as follows:

$$\delta = \frac{\omega_{max} - \omega_{min}}{\omega_{avg}}$$

$$\xi = \frac{\Delta W_{max} + |\Delta W_{min}|}{imep \cdot V_d} = \frac{\Delta W_{tot}}{imep \cdot V_d}$$

$\delta$  is a design parameter and sets the limit to the maximum allowed speed fluctuation. In this study it is accepted a fluctuation of the 1%, therefore:

$$\delta = 0.01$$

On the other hand,  $\xi$  is not predetermined; however, it can be calculated by evaluating the difference between the shaft work and the resistant work at the maximum and minimum instantaneous crankshaft speeds. These two contributions to work can be determined by integrating their respective moments over the crank angle period. The so evaluated quantities, normalized with respect to the unitary displacement, are reported in Figure 9, along with tangential and resistant pressure.

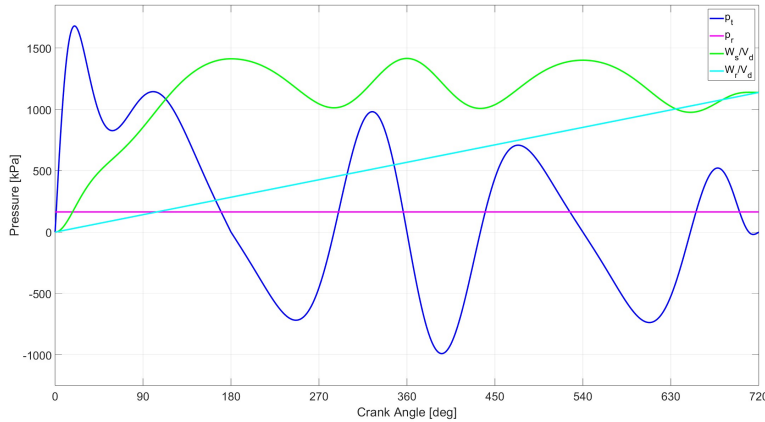


Figure 9: Work and pressure contributions

It is important to note that, as previously mentioned, under steady-state conditions, the rotational speed of the engine at the beginning and end of the cycle remains equal. Consequently, the shaft work and resistant work at the end of the cycle are also equal. As illustrated in Figure 9, this condition is satisfied, thereby confirming the validity of both the analysis and the results.

Once the functions of shaft and resistant work are obtained,  $\Delta W_{max}$  and  $\Delta W_{min}$  can be simply evaluated as the maximum and minimum value of:

$$\Delta W(\theta) = W_s(\theta) - W_r(\theta) \quad (40)$$

from which:

$$|\Delta W_{max}| = 353.4 \text{ J}$$

$$|\Delta W_{min}| = 17.46 \text{ J}$$

After evaluating  $\Delta W_{max}$  and  $\Delta W_{min}$ , the coefficient  $\xi$  is computed:

$$\xi = 1.1528$$

and therefore, form Equation 39:

$$J = 0.0939 \text{ kg} \cdot \text{m}^2$$

Once the engine and total inertia are determined, the flywheel's inertia can then be calculated, therefore:

$$J_{flw} = 0.0935 \text{ kg} \cdot \text{m}^2$$

Once calculated the total rotational inertia, its diameter can be determined as a consequence, through the following equation:

$$J_{flw} = \frac{\pi}{32} \cdot \rho \cdot w_f \cdot D_f^4 \quad (41)$$

Since both  $w_f$  and  $D_f$  are unknown, the equation cannot be solved directly. Therefore, an additional equation is required. Specifically:

$$w_f = \frac{D_f}{10} \quad (42)$$

Thus, the following flywheel diameter for a single cylinder engine is obtained:

$$D_f = 0.262 \text{ m}$$

Since the evaluated diameter stay within the range  $2S < D_f < 5S$ , no further modifications are required.

### 3.4 Calculation of the instantaneous crankshaft speed

Integrating the equation of the shaft's dynamic equilibrium between  $\theta = 0$  and a generic crank angle  $\theta$ , it is possible to derive an expression for the angular velocity  $\omega(\theta)$  at each crank angle position, as shown below:

$$\omega(\theta) = \sqrt{\omega_0^2 + \frac{2}{J}(W_s(\theta) - W_r(\theta))} \quad (43)$$

Since  $\omega(\theta)$  is unknown, the initial value  $\omega_0$  is also unknown. Therefore, to evaluate the instantaneous angular velocity function, an iterative procedure is employed. This procedure continues until the average value of the instantaneous angular velocity matches the desired value, i.e. the engine speed considered in this analysis.

The initial guess for  $\omega_0$  is set equal to  $\omega_{avg}$ , and the first iteration  $\omega_I(\theta)$  is computed. Then, the error between the average value of  $\omega_I(\theta)$  and the desired value is calculated as:

$$s = \omega_{avg,I} - \omega_{avg} \quad (44)$$

In the second iteration, the updated value of  $\omega_0$  is computed as:

$$\omega_{II,0} = \omega_{I,0} + s \quad (45)$$

The new instantaneous angular velocity is then recalculated. The final result is shown in Figure 10 in red, along with the result of the first iteration.

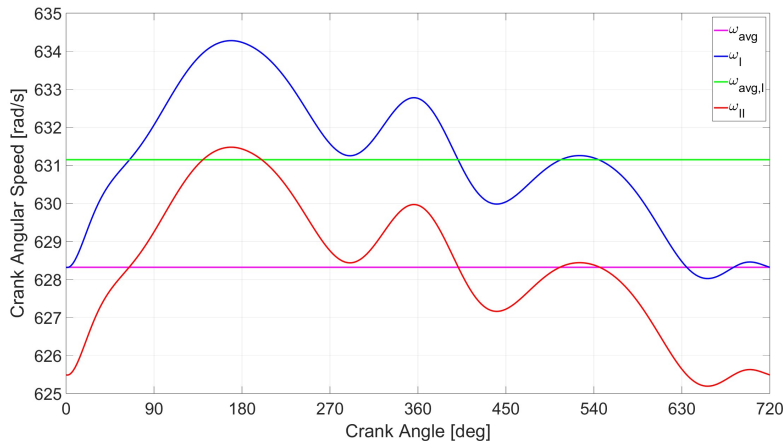


Figure 10: Instantaneous shaft speed

## 4 Multi-cylinder engine

For the multi-cylinder case, a 4 cylinder engine is considered, having the same air-fuel cycle calculated for the single cylinder engine. Moreover, a non variant cycle is considered among all the cylinders.

#### 4.1 Calculation of the shaft and resistant moment

In order to evaluate the total moment acting on the crankshaft in a multi cylinder engine, we need to sum up the contributions provided by each cylinder, considering the phase shift among them and the firing order, which in the analyzed case is the following: 1-3-4-2. Additionally, the phase shift is evaluated as follows:

$$\Delta\phi = \frac{m \cdot 360}{i} \quad (46)$$

where  $i$  is the number of cylinders and  $m$  is the number of revs/cycle. Since in this survey a 4T 4-cylinders engine is considered,  $m = 2$  and  $i = 4$ .

Therefore the value of the phase shift is found:

$$\Delta\phi = 180^\circ \text{CA}$$

In Figure 11, the tangential pressure resulting from the overall superposition effect of the four cylinders is presented, along with the individual tangential pressure profiles of each cylinder.

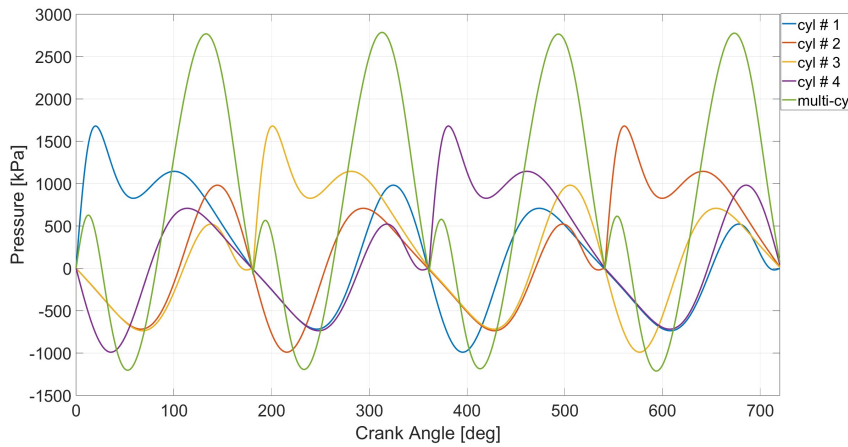


Figure 11: Contributions of the different cylinders in the overall tangential pressure

#### 4.2 Calculation of the flywheel diameter

As for the single cylinder engine, the flywheel diameter is evaluated by using the kinematic and dynamic irregularity. However, differently from the kinematic irregularity which remains constant, the dynamic one is evaluated taking into account the increase of the overall displacement. Therefore, the new equation is the following:

$$\xi = \frac{\Delta W_{max,multi} + |\Delta W_{min,multi}|}{imep \cdot iV_d} = \frac{\Delta W_{tot,multi}}{imep \cdot iV_d}$$

Similarly to the single cylinder engine,  $\Delta W_{max}$  and  $\Delta W_{min}$  are evaluated by computing the difference between the crankshaft and resistant work, shown in Figure 12 along with tangential and resistant pressure.

The following values are obtained:

$$|\Delta W_{max}| = 10.36 \text{ J}$$

$$|\Delta W_{min}| = 262.7 \text{ J}$$

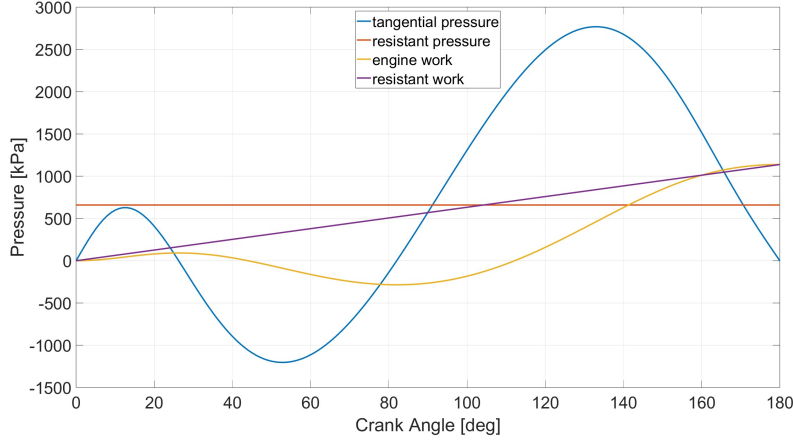


Figure 12: Work and pressure contributions in the multi-cylinder engine

Hence,  $\xi$  can be computed:

$$\xi = 0.2122$$

The accuracy of the analysis can be verified by examining the dynamic irregularities of single-cylinder and multi-cylinder engines. The calculations are considered correct if the condition  $\xi_{multi} < \frac{\xi_{single}}{i}$  is satisfied. Based on the results obtained, this condition is met, confirming the validity of the analysis.

Once the dynamic irregularity is evaluated, the total inertia of the system can be computed with the following equation:

$$J_{multi} = \frac{\xi_{multi} \cdot imep \cdot iV_d}{\delta \cdot \omega_{avg}^2} \quad (47)$$

from which:

$$J_{multi} = 0.0692 \text{ kg} \cdot \text{m}^2$$

Once the engine and total inertia of the multi-cylinder engine are determined, the flywheel's inertia can then be calculated, therefore:

$$J_{flw,multi} = 0.0675 \text{ kg} \cdot \text{m}^2$$

Once calculated the total rotational inertia, its diameter can be determined as a consequence, through the following equation:

$$D_{f,multi} = \sqrt[5]{\frac{320 \cdot J_{flw,multi}}{\rho \cdot \pi}} \quad (48)$$

from which:

$$D_{f,multi} = 0.246 \text{ m}$$

It is crucial to ensure that the flywheel diameter in the multi-cylinder engine is smaller than that of the single-cylinder engine, as this reflects the efficiency and balance achieved through the distribution of forces in the multi-cylinder configuration. A reduced flywheel diameter indicates that the multi-cylinder engine experiences lower fluctuations in rotational speed, leading to smoother operation and reduced dynamic irregularities. This improvement is a direct result of the overlapping power strokes in the multi-cylinder engine, which distribute the load more evenly over the cycle.

By meeting the condition  $D_{f,multi} < D_{f,single}$ , the analysis confirms the effectiveness of the multi-cylinder design in minimizing rotational irregularities and optimizing the engine's overall functionality.

### 4.3 Calculation of the instantaneous crankshaft speed

The same iterative procedure applied in the evaluation of the instantaneous rotational speed of the single cylinder engine can be applied also for the multi-cylinder engine, leading to the rotational speed plot reported in Figure 13.

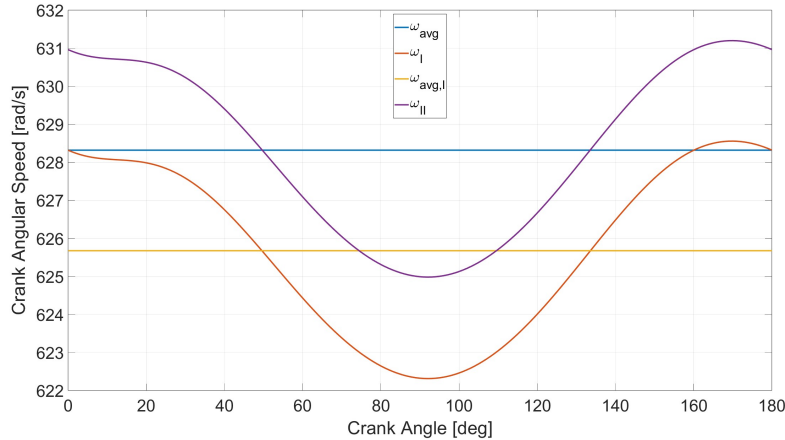


Figure 13: Instantaneous shaft speed of the multi-cylinder engine

## 5 Conclusions

In this study, the design and dimensioning of the flywheel for a naturally aspirated spark ignition engine were thoroughly examined. The analysis covered both single-cylinder and multi-cylinder configurations, focusing on key parameters such as thermodynamic cycle characteristics, inertia, and dynamic irregularities.

The single-cylinder engine's flywheel diameter was determined to be:

$$D_{f,single} = 0.262\text{m}$$

while for the multi-cylinder engine, the diameter was optimized to:

$$D_{f,multi} = 0.246\text{m}$$

These results reflect the reduced dynamic irregularities achieved in the multi-cylinder engine due to the distribution of forces across multiple power strokes.

The findings underline the importance of accurate thermodynamic and dynamic analysis in engine design, ensuring both operational efficiency and mechanical stability. Moreover, the iterative methods employed for determining crankshaft speeds provided precise insights into angular velocity fluctuations, further enhancing the robustness of the analysis.

## 6 Appendix

```
1 clear all
2 close all
3 clc
4
5 %% A-F CYCLE
6
7 S = 78.95e-3;
8 B = 70.8e-3;
9 Lambda = 0.306;
10 r = S/2;
11 rc = 11;
12 Vd = pi/4 * B^2 * S;
13 Vc = Vd / (rc - 1);
14 m = 1.35;
15 m_1 = 1.27;
16
17 p1 = 88.5;
18 p2 = 2253;
19 p3 = 8587;
20 p4 = 408.6;
21 p6 = 100;
22 p7 = p1;
23 V1 = rc * Vc;
24
25 theta_deg = linspace(0, 360, 361);
26 theta = theta_deg * pi/180;
27 beta = asin(Lambda * sin(theta));
28 x = r * ((1-cos(theta)) + 1/Lambda * (1-cos(beta)));
29 Vx = Vc + x * pi/4 * B^2;
30 p_2 = p1 .* (V1./Vx).^m;
31 p_4 = p3 .* (Vc./Vx).^m_1;
32
33 figure;
34 plot(Vx, p_2, 'LineWidth', 3, 'Color', 'blue')
35 hold on;
36 plot([Vc Vc], [p2 p3], 'LineWidth', 3, 'Color', 'blue')
37 hold on;
38 plot(Vx, p_4, 'LineWidth', 3, 'Color', 'blue')
39 hold on;
40 plot([V1 V1], [p4 p6], 'LineWidth', 3, 'Color', 'blue')
41 hold on;
42 plot([Vc Vc], [p6 p7], 'LineWidth', 3, 'Color', 'blue')
43 hold on;
44 plot([Vc V1], [p7 p1], 'LineWidth', 3, 'Color', 'blue')
45 hold on;
46 plot([Vc V1], [p6 p6], 'LineWidth', 3, 'Color', 'blue')
47 title('a-f cycle')
48 xlabel('Volume [m^3]')
49 ylabel('Pressure [kPa]')
50 grid on;
51
52 %% GAS PRESSURE
53
54 theta_34 = linspace(0, 180, 181);
55 theta_56 = linspace(180, 360, 181);
56 p_6 = p6 * ones(size(theta_56));
57 theta_71 = linspace(360, 540, 181);
58 p_7 = p1 * ones(size(theta_71));
59 theta_12 = linspace(540, 720, 181);
60
61 figure;
62 theta_totale = [theta_34, theta_56, theta_71, theta_12];
63 p_totale = [p_4(1:181), p_6, p_7, p_2(181:361)];
64
```

```

65 plot(theta_totale, p_totale, 'LineWidth', 3, 'Color', 'blue');
66 %title('Gas pressure')
67 xlabel('Crank Angle [deg]')
68 ylabel('Pressure [kPa]')
69 xlim([0, 720])
70
71 %% EFFECTIVE PRESSURE
72
73 m_rec_Vd = 1.2e3;
74 n = 6000;
75 u = 2*S*n/60;
76 p_amb = 100;
77
78 theta_34_rad = theta_34 * pi/180;
79 p_inertia_34 = -m_rec_Vd * pi^2*u^2/2*(cos(theta_34_rad)+Lambda*cos(2*
    theta_34_rad));
80 p_inertia_34 = p_inertia_34 * 10^-3; % Pa to kPa
81 p_eff_34 = p_4(1:181) - p_amb + p_inertia_34;
82
83 theta_56_rad = theta_56 * pi/180;
84 p_inertia_56 = -m_rec_Vd * pi^2*u^2/2*(cos(theta_56_rad)+Lambda*cos(2*
    theta_56_rad));
85 p_inertia_56 = p_inertia_56 * 10^-3;
86 p_eff_56 = p_6 - p_amb + p_inertia_56;
87
88 theta_71_rad = theta_71 * pi/180;
89 p_inertia_71 = -m_rec_Vd * pi^2*u^2/2*(cos(theta_71_rad)+Lambda*cos(2*
    theta_71_rad));
90 p_inertia_71 = p_inertia_71 * 10^-3;
91 p_eff_71 = p_7 - p_amb + p_inertia_71;
92
93 theta_12_rad = theta_12 * pi/180;
94 p_inertia_12 = -m_rec_Vd * pi^2*u^2/2*(cos(theta_12_rad)+Lambda*cos(2*
    theta_12_rad));
95 p_inertia_12 = p_inertia_12 * 10^-3;
96 p_eff_12 = p_2(181:361) - p_amb + p_inertia_12;
97
98 p_eff_totale = [p_eff_34(1:180), p_eff_56(1:180), p_eff_71(1:180), p_eff_12
    ];
99 p_inertia_totale = [p_inertia_34(1:180), p_inertia_56(1:180), p_inertia_71
    (1:180), p_inertia_12];
100 theta_totale = (0:1:720);
101
102 hold on;
103 plot(theta_totale, p_eff_totale, 'LineWidth', 3, 'Color', 'magenta')
104 hold on;
105 plot(theta_totale, p_inertia_totale, 'LineWidth', 3, 'Color', 'green')
106 hold on;
107 plot([0 720], [p_amb p_amb], 'LineWidth', 3, 'Color', 'cyan')
108 grid on;
109 lgd = legend('gas pressure', 'effective pressure', 'inertia pressure',
    'crankcase pressure');
110
111 %% INERTIA PRESSURE PLOT
112
113 figure;
114 plot(Vx, p_2, 'LineWidth', 3, 'Color', 'blue')
115 hold on;
116 plot(Vx(1:181), -p_inertia_totale(1:181), 'LineWidth', 3, 'Color', 'red');
117 hold on;
118 plot([Vc Vc], [p2 p3], 'LineWidth', 3, 'Color', 'blue')
119 hold on;
120 plot(Vx, p_4, 'LineWidth', 3, 'Color', 'blue')
121 hold on;
122 plot([V1 V1], [p4 p6], 'LineWidth', 3, 'Color', 'blue')
123 hold on;

```

```

124 plot([Vc Vc], [p6 p7], 'LineWidth', 3, 'Color', 'blue')
125 hold on;
126 plot([Vc V1], [p7 p1], 'LineWidth', 3, 'Color', 'blue')
127 hold on;
128 plot([Vc V1], [p6 p6], 'LineWidth', 3, 'Color', 'blue')
129 xlabel('Volume [m^3]')
130 ylabel('Pressure [kPa]')
131 grid on;
132 lgd = legend('a-f cycle', 'p_{in}');
133
134 %% TANGENTIAL PRESSURE
135
136 theta_totale_rad = theta_totale * pi/180;
137 beta_totale_rad = asin(Lambda * sin(theta_totale_rad));
138 p_t = p_eff_totale .* sin(beta_totale_rad + theta_totale_rad) ./ cos(
    beta_totale_rad);
139
140 figure;
141 plot(theta_totale, p_t, 'LineWidth', 3, 'Color', 'blue')
142 xlabel('Crank Angle [deg]')
143 ylabel('Pressure [kPa]')
144 xlim([0, 720])
145 ylim([-1250 1850])
146 title('Tangential Pressure')
147 xticks(0:90:720);
148 grid on;
149
150 %% CRANKSHAFT AND RESISTANT MOMENTUM/WORK
151
152 imep = 10.35e5;      %[Pa]
153
154 Ms = p_t * Vd/2 * 10^-3;      %[Nm]
155 Mr = imep/(2*pi) * Vd/2;      %[Nm]
156 p_r = imep/(2*pi)*10^-3;    %[kPa]
157
158 Ws = cumtrapz(theta_totale*pi/180, Ms);
159 Wr = theta_totale*pi/180*Mr;
160
161 Ws_Vd = Ws/Vd * 10^-3;    %[kPa]
162 Wr_Vd = Wr/Vd * 10^-3;    %[kPa]
163
164 Delta_W = Ws - Wr;
165 Delta_W_max = abs(max(Delta_W));
166 Delta_W_min = abs(min(Delta_W));
167
168 figure;
169 plot(theta_totale, p_t, 'LineWidth', 3, 'Color', 'blue');
170 hold on;
171 plot([0 720], [p_r p_r], 'LineWidth', 3, 'Color', 'magenta');
172 hold on;
173 plot(theta_totale, Ws_Vd, 'LineWidth', 3, 'Color', 'green');
174 hold on;
175 plot(theta_totale, Wr_Vd, 'LineWidth', 3, 'Color', 'red');
176 xlabel('Crank Angle [deg]')
177 ylabel('Pressure [kPa]')
178 xlim([0, 720])
179 ylim([-1250 1850])
180 xticks(0:90:720);
181 grid on;
182 lgd = legend('p_t', 'p_r', 'W_s/V_d', 'W_r/V_d');
183
184 %% FLYWHEEL DIAMETER
185
186 delta = 0.01;
187 mrot_Vd = 0.85e3;
188 ro = 7.7e3;

```

```

189 zeta = (Delta_W_max + Delta_W_min)/(imep * Vd);
190 Jtot = zeta*imep*Vd/(delta * (n*pi/30)^2);
191 Jeng = mrot_Vd * Vd * r^2;
192
193 Jflw = Jtot - Jeng;
194
195 Dflw = (320*Jflw/(ro*pi))^(1/5);
196
197 %% CRANKSHAFT SPEED
198
199 omega_avg = n*pi/30;
200
201 omega_1_0 = omega_avg;
202 omega_1 = sqrt(omega_1_0^2 + 2/Jtot*(Ws-Wr));
203 avg_omega_1 = mean(omega_1);
204
205 s = omega_1_0 - avg_omega_1;
206 omega_2_0 = s + omega_1_0;
207 omega_2 = sqrt(omega_2_0^2 + 2/Jtot*(Ws-Wr));
208 avg_omega_2 = mean(omega_2);
209
210
211 figure;
212 plot([0 720], [omega_1_0 omega_1_0], 'LineWidth', 3, 'Color', 'magenta');
213 hold on;
214 plot(theta_totale, omega_1, 'LineWidth', 3, 'Color', 'blue')
215 hold on;
216 plot([0 720], [avg_omega_1 avg_omega_1], 'LineWidth', 3, 'Color', 'green');
217 hold on;
218 plot(theta_totale, omega_2, 'LineWidth', 3, 'Color', 'red');
219 xlabel('Crank Angle [deg]')
220 ylabel('Crank Angular Speed [rad/s]')
221 xlim([0, 720])
222 xticks(0:90:720);
223 grid on;
224 lgd = legend('\omega_{avg}', '\omega_I', '\omega_{avg,I}', '\omega_{III}')
225 ;
226
227
228 %% MULTI-CYLINDER ENGINE
229
230
231 %% CRANKSHAFT AND RESISTANT MOMENTUM/WORK
232
233 % TANGENTIAL PRESSURE
234 p_t1 = p_t;
235 p_t2 = [p_t(181:360) p_t(361:540) p_t(541:721) p_t(1:180)];
236 p_t3 = [p_t(541:721) p_t(1:180) p_t(181:360) p_t(361:540)];
237 p_t4 = [p_t(361:540) p_t(541:721) p_t(1:180) p_t(181:360)];
238 p_t_multi = p_t1 + p_t2 + p_t3 + p_t4;
239
240 figure;
241 plot(theta_totale, p_t1, 'LineWidth', 3);
242 hold on;
243 plot(theta_totale, p_t2, 'LineWidth', 3);
244 hold on;
245 plot(theta_totale, p_t3, 'LineWidth', 3);
246 hold on;
247 plot(theta_totale, p_t4, 'LineWidth', 3);
248 hold on;
249 plot(theta_totale, p_t_multi, 'LineWidth', 3);
250 xlabel('Crank Angle [deg]')
251 ylabel('Pressure [kPa]')
252 xlim([0, 720])
253 xticks(0:90:720);

```

```

254 grid on;
255 lgd = legend('cyl # 1', 'cyl # 2', 'cyl # 3', 'cyl # 4', 'multi-cyl');
256
257 % RESISTANT PRESSURE
258 p_r_multi = p_r * 4;
259
260 figure;
261 plot(theta_totale, p_t_multi, 'LineWidth', 3);
262 hold on;
263 plot([0 720], [p_r_multi p_r_multi], 'LineWidth', 3);
264
265 % SHAFT AND RESISTANT WORK
266
267 Ms_multi = p_t_multi * Vd/2 * 10^3;      %[Nm]
268 Mr_multi = p_r_multi * Vd/2 * 10^3;      %[Nm]
269
270 Ws_multi = cumtrapz(theta_totale*pi/180, Ms_multi);
271 Wr_multi = theta_totale*pi/180*Mr_multi;
272
273 Ws_Vd_multi = Ws_multi/Vd * 10^-3;    %[kPa]
274 Wr_Vd_multi = Wr_multi/Vd * 10^-3;    %[kPa]
275
276 hold on;
277 plot(theta_totale, Ws_Vd_multi, 'LineWidth', 3)
278 hold on;
279 plot(theta_totale, Wr_Vd_multi, 'LineWidth', 3)
280 xlabel('Crank Angle [deg]')
281 ylabel('Pressure [kPa]')
282 xlim([0, 180])
283 xticks(0:20:180);
284 grid on;
285 lgd = legend('tangential pressure', 'resistant pressure', 'engine work', 'resistant work');
286
287 Delta_W_multi = Ws_multi - Wr_multi;
288 Delta_W_max_multi = abs(max(Delta_W_multi));
289 Delta_W_min_multi = abs(min(Delta_W_multi));
290
291 %% FLYWHEEL DIAMETER
292
293 zeta_multi = (Delta_W_max_multi + Delta_W_min_multi)/(imep * 4 * Vd);
294 Jtot_multi = zeta_multi*imep*4*Vd/(delta * (n*pi/30)^2);
295 Jeng_multi = Jeng * 4;
296
297 Jflw_multi = Jtot_multi - Jeng_multi;
298
299 Dflw_multi = (320*Jflw_multi/(ro*pi))^(1/5);
300
301 %% %% CRANKSHAFT SPEED
302
303 omega_avg = n*pi/30;
304
305 omega_1_0 = omega_avg;
306 omega_1 = sqrt(omega_1_0^2 + 2/Jtot_multi*(Ws_multi-Wr_multi));
307 avg_omega_1 = mean(omega_1);
308
309 s = omega_1_0 - avg_omega_1;
310 omega_2_0 = s + omega_1_0;
311 omega_2 = sqrt(omega_2_0^2 + 2/Jtot_multi*(Ws_multi-Wr_multi));
312 avg_omega_2 = mean(omega_2);
313
314 figure;
315 plot([0 720], [omega_1_0 omega_1_0], 'LineWidth', 3);
316 hold on;
317 plot(theta_totale, omega_1, 'LineWidth', 3)
318 hold on;

```

```

319 plot([0 720], [avg_omega_1 avg_omega_1], 'LineWidth', 3);
320 hold on;
321 plot(theta_totale, omega_2, 'LineWidth', 3);
322 xlabel('Crank Angle [deg]')
323 ylabel('Crank Angular Speed [rad/s]')
324 xlim([0, 180])
325 xticks(0:20:180);
326 grid on;
327 lgd = legend('\omega_{avg}', '\omega_I', '\omega_{avg,I}', '\omega_{III}')
      ;

```